A Direct Drive Rotary Valve for Efficient Power Generation in Gas Expander Based Small Scale Power Plants

Md Shazzad Hossain*, Truong Phung, Apurv Kumar, Ibrahim Sultan
Institute of Innovation, Science and Sustainability | Federation University Australia
ss.hossain@federation.edu.au, t.phung@federation.edu.au,
apurv.kumar@federation.edu.au,i.sultan@federation.edu.au
* Corresponding author

***Abstract*— Organic Rankine Cycle (ORC) based small-scale energy generation systems can be utilized to address the rapidly increasing demand for low-cost power. But the overall efficiency of these systems is limited by the efficiency of the gas expander which extracts work from the working fluid. This efficiency can be greatly improved by regulating the flow of working fluid into the expander chamber using a control valve. In this manuscript, a rotary valve driven by a direct drive stepper motor (DDRV) is proposed and the dynamics of the valve is studied. The overall performance of the limaçon expander equipped with this valve on the inlet port is also analyzed. The thermodynamic performance of the system such as isentropic efficiency and filling factor are calculated. An increase in isentropic efficiency of 14.86% with a decrease in filling factor of 16.88% is achieved compared to the ported, without an inlet valve, expander.**

***Keywords*—** Limaçon gas expander; Rotary machine; Energy conversion; Direct Drive Rotary Valve (DDRV); Control valve; System efficiency; Waste heat recovery

I. Introduction

The adverse effects of climate change and global warming are mainly associated with energy generation activities. This could be addressed by improving the efficiency of the current energy conversion processes. Currently, conventional power generation from coal, oil, or natural gas has an overall efficiency in the range of 30-40% being limited by the low efficiency of turbines, boilers, and condensers [1]. The efficiency can be raised to 55% in the combined cycle arrangement [1]. Even then, about 45% of the energy in the form of heat is wasted which could have been converted to electricity using proper means.

One way to minimize the wastage of energy is to maximize the use of low-grade or waste heat. This can be done by introducing a Waste Heat Recovery system (WHR) where the low-temperature heat resources can be converted to power using an Organic Rankine Cycle (ORC). ORC-WHR systems can operate at temperatures as low as 73.3°C which make them a great tool to improve the efficiencies of a wide range of thermal cycles [2][3]. ORC-WHR systems are also cost-effective compared to similar energy conversion technologies[4]. In recent times, many small-scale ORC based systems suitable for domestic use have been developed. These ORC-based systems are ideal for home-based power generation due to their lower, therefore, safer operating temperatures and pressures. Quoilin *et al.* reported a 1-kWe off-grid solar thermal ORC system installed in rural Lesotho and found that it is producing clean energy at a lower cost compared to diesel generators ($0.18 less per kWh)[5]. These small-scale ORC-based systems can also be utilized as combined heat and power (CHP) systems to provide power generation as well as heat using diverse renewable energy sources i.e., solar, geothermal, and biomass to name a few. [6]–[8]. Despite their huge potential, the lack of efficient expanders in these systems restricts their use in the wider domain.

The overall ORC system efficiency, in general, is within the range of 9.6% to 18.1%; this depends on various factors such as the types of working fluid used, the efficiency of the expander, and the evaporator and condenser temperatures [9]. The overall performance of an ORC system is highly sensitive to the isentropic efficiency of the expander. Sultan *et al.* proposed a heat recovery and power generation technique using a limaçon expander and showed that the employment of a cam-operated inlet control valve has the potential to increase the overall performance of the expander by 24% [10], [11]. However, these cam-based valves have fixed characteristics and the independent motion of the cam and cannot be flexibly adjusted to match the change of the load or operating conditions.

Stepper motors valve lend themselves to the flexibility in arrangement and the controllability which can be programmed to open or close at any angle of rotation of the expander rotor. Hence, in this manuscript, a stepper-motor-operated valve is proposed in place of a cam-operated one. The valve as well as expander performance will be studied to realise the potential of such a valve in WHR applications. Stepper motor is chosen for this task because of its high precision controllability and other beneficial features such as a low cost and high torque package. A stepper motor is similar to a synchronous motor whose rotor is able to produce precise discrete rotational motions from a sequence of electric pulses at its stator. The direction and angle of the rotation and angular speed can be controlled by varying the order of input pulses. There are mainly three types of stepper motors, namely: variable reluctance, permanent magnet, and hybrid; of note is that the hybrid stepper motors offer better performance compared to the other two [12]. The mathematical model of the stepper motor and valve will be detailed in section III below.

II. Outline of the proposed DDRV

The proposed direct drive rotary valve (DDRV), illustrated in Fig. 1, has a rotating spool with an orifice cut out through the middle for the fluid passage. In this DDRV the valve spool is rotated by a stepper motor. This valve is designed such that it is in a normally open position (NO) when the stepped motor is at its initial position or idle. This NO operation of the valve ensures that the flow of working fluid to the connected gas expander will not be interrupted due to unforeseeable mechanical failure in the valve and thus the expander remains operational. When the valve angular position $\theta = 0$, the compressed fluid at a pressure P_{in} goes through the valve opening and flows into the valve antechamber at a pressure P_a. To close the valve, an electromagnetic torque, τ_e generated by the stepper motor rotates the valve spool in the clockwise direction with an angular velocity ω and stops at an angle θ_{max} thereby fully blocking the flow. Likewise, during the valve transition from close to open positions, the motor is rotated in the counter-clockwise direction, when $\theta = 0$ the valve settles down at its initial NO position.

III. Mathematical Modelling

In this section, a detailed mathematical model of the stepper motor-operated valve will be formulated starting with the stepper motor model followed by a model of the associated valve dynamics.

* This project is supported by Destination Australia and Federation University Research Excellence Scholarships

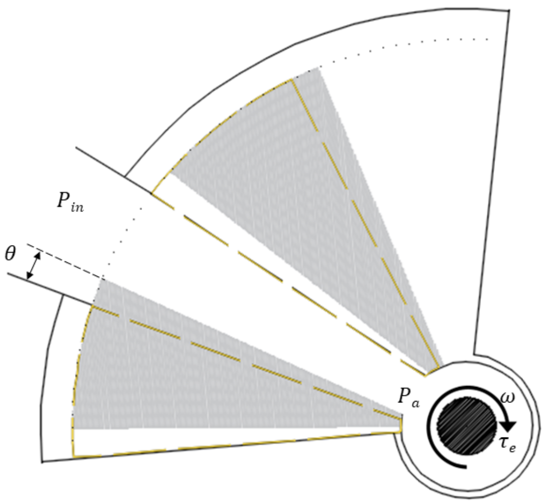

Figure 1: A proposed direct-drive stepper motor valve (DDRV)

A. Stepper Motor Model

A stepper motor is a high-torque synchronous motor that converts electric pulses into specific and incremental movements. The sequence of electric pulse input determines the direction of the rotor shaft's rotation. The speed and angle of the rotation are also controlled by these input pulses. For the purpose of this manuscript, a two-phase hybrid-type stepper motor will be utilized. The mathematical model of a stepper motor consists of electrical and mechanical sub-models. The voltage and current relationships in the two phases a and b can be modelled by a simple RL circuit incorporating the rate of change of flux linkages or otherwise called induced electromotive force (emf) as shown in equations (1a) and (1b) [13]:

$$V_a = R_s i_a + \frac{d}{dt}(L_a i_a + \psi_{ma}) \tag{1a}$$

$$V_b = R_s i_b + \frac{d}{dt}(L_b i_b + \psi_{mb}) \tag{1b}$$

where V and i denote voltage V and current A, respectively; $R_s(\Omega)$ is the stator resistance; and $L(H)$ is the inductance. The mutual flux linkages ψ_{ma} and ψ_{mb} in phase a and b are given by Iqteit et al. [14] as $\psi_{ma} = \psi_m cos(p\theta)$ and $\psi_{mb} = \psi_m sin(p\theta)$, respectively; where p is the number of pole pairs in the rotor given in equation (2) below and θ is the rotor angular displacement measured in degrees.

$$p = \frac{360}{2m \times \theta_s} \tag{2}$$

where m is the number of phases and $\theta_s(^\circ)$ is the step angle of the motor. The maximum flux linkage ψ_m can be experimentally calculated using equation (3) by running the motor at a constant speed n and measuring the open circuit winding voltage E_m [14] as below

$$\psi_m = \frac{30 \times E_m}{n\pi} \tag{3}$$

The self inductances L_a and L_b are given by Iqteit et al. [14] as functions of average permeance, $\bar{P}$ (H), and the number of teeth per stator pole, N_s as $L_s = L_a = L_b = 4\bar{P}N_s^2$. Substituting the expressions for ψ_{ma} and ψ_{mb} in (1a) and (1b), respectively, give

$$V_a = R_s i_a + L_s \frac{di_a}{dt} - p\psi_m sin(p\theta)\frac{d\theta}{dt} \tag{4a}$$

$$V_b = R_s i_b + L_s \frac{di_b}{dt} + p\psi_m cos(p\theta)\frac{d\theta}{dt} \tag{4b}$$

For simplification of analysis and ease of control implementation, the voltage-current equations (1a) and (1b) in two-axis orthogonal stationary reference a and b are transformed into $d-q$ rotating reference axes using the well-known Park transformation as given below [15]:

$$\begin{bmatrix} V_d \\ V_q \end{bmatrix} = \begin{bmatrix} cos(p\theta) & sin(p\theta) \\ -sin(p\theta) & cos(p\theta) \end{bmatrix} \begin{bmatrix} V_a \\ V_b \end{bmatrix} \tag{5}$$

where, $[T_p] = \begin{bmatrix} cos(p\theta) & sin(p\theta) \\ -sin(p\theta) & cos(p\theta) \end{bmatrix}$ is the Park transformation matrix. Similar expressions for current transformation also hold true.

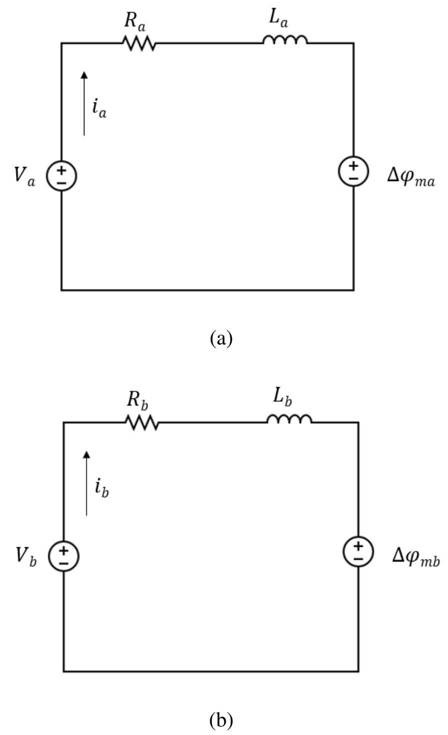

Figure 2: Equivalent circuit of a hybrid stepper motor for (a) phase a and (b) phase b

Transforming the voltage-current relationships in stationary axis $a-b$ in equation (4a) and (4b) into $d-q$ synchronously rotating axis using the above transformation gives 6 according to Yang & Kuo [16] as follow

$$\begin{bmatrix} V_d \\ V_q \end{bmatrix} = \begin{bmatrix} R_s + L_s\Delta & -p\omega L_s \\ p\omega L_s & R_s + L_s\Delta \end{bmatrix} \begin{bmatrix} i_d \\ i_q \end{bmatrix} + p\psi_m\omega \begin{bmatrix} 0 \\ 1 \end{bmatrix} \tag{6}$$

where $\omega = \frac{d\theta}{dt}$ is the angular velocity of the motor. The electromagnetic torque produced by the motor can be deduced from its power intake. The input electrical power, P_{in}, supplied to the motor can be expressed as:

$$\begin{aligned} P_{in} &= V_d i_d + V_q i_q \\ &= R_s(i_d^2 + i_q^2) + \frac{1}{2}L_s\frac{d}{dt}(i_d^2 + i_q^2) + p\psi_m\omega i_q \\ &= P_{cu} + P_{ind} + P_{mech} \end{aligned} \tag{7}$$

where P_{cu} is the copper loss due to current flow in the motor conductor, P_{ind} is the power component corresponding to magnetic stored energy in the coils, and P_{mech} is the mechanical power. Consequently, the electromagnetic torque is given by 8.

$$\tau_e = \frac{P_{mech}}{\omega} = p\psi_m i_q \tag{8}$$

B. Valve Dynamics

The dynamics of the valve can be modelled by the following equation of motion:

$$\tau_e = J\frac{d\omega}{dt} + B\omega + \tau_f + \tau_l \tag{9}$$

where J is the total inertia $(kg.m^2)$ of motor and associated valve spool, B is viscous friction coefficient $(Nm.s)$, τ_f is steady state flow torque (Nm), and τ_l is the loading torque (Nm). The flow torque τ_f is due to the flow of fluid through the valve port. When fluid passes through the valve port, it introduces a flow force on the rotating valve spool. The axial component of this force produces a torque on the spool which obstructs the movement of the spool. The expression of flow torque is given by Okhotnikov et al. [17] as below

$$\tau_f = 2C_d C_v(P_{in} - P_a)A(\theta) r sin\alpha \tag{10}$$

where C_d is the discharge coefficient, C_v is the discharge velocity coefficient, $A(\theta)$ is the dynamic area of the orifice, r is the radius of the rotating spool from the centre of rotation and α is the angle between radial flow direction and radius of the rotating spool denoted as the jet angle. Fig. 3 shows the variation of passage area, $A(\theta)$, which can be expressed as a function of θ as shown below

$$A(\theta) = D_{valve}D_{orifice}(\theta_{max} - \theta) \tag{11}$$

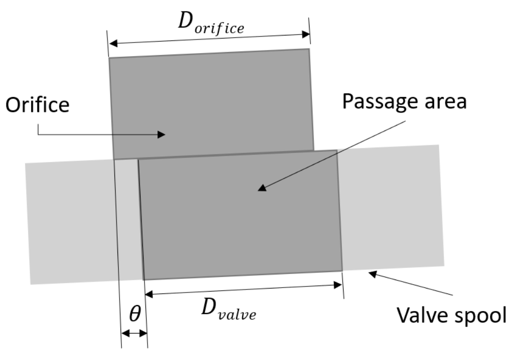

Figure 3: Dynamic passage area

Substituting 11 into 10 gives the expression of flow torque as follows:

$$\tau_f = 2rC_dC_vD_{valve}D_{orifice}\Delta\theta(P_{in} - P_a)sin\alpha \tag{12}$$

where $\Delta\theta = (\theta_{max} - \theta)$.

The flow rate through the orifice is given by Watton [18] is shown below

$$q_l = C_dA(\theta)\sqrt{\frac{1}{\rho}(P_{in} - \frac{\theta}{\mid\theta\mid}P_a)} \tag{13}$$

IV. Simulation of Direct Drive Rotary Valve (DDRV)

The simulation of the proposed DDRV is carried out in two steps beginning with the simulation of the dynamic response characteristics followed by the simulation of its application in a gas expander. As the proposed valve is primarily designed to be used in a gas expander system, the simulation is done with respect to the expander rotor angle rather than time. For this purpose, a limaçon-to-circular (L2C) expander as shown in Fig. 4 and proposed by Sultan is selected for the study [19].

The valve is designed in such a way that it can allow and block the flow of working fluid to the expander chamber at precise angular positions of the machine rotor. Fig. 5 depicts the operation of the proposed DDRV with reference to the expander rotor angular positions. The two important angular positions are termed cutoff angle and pass angle, as shown in Fig. 5. The cutoff angle is the angular position of the expander rotor at which the valve will operate to cutoff flow into the expander. Contrarily, the pass angle is the angular position of the rotor at which the valve will operate to resume flow into the expander. The angular position of the rotor can be measured directly using an appropriate sensor or can be estimated

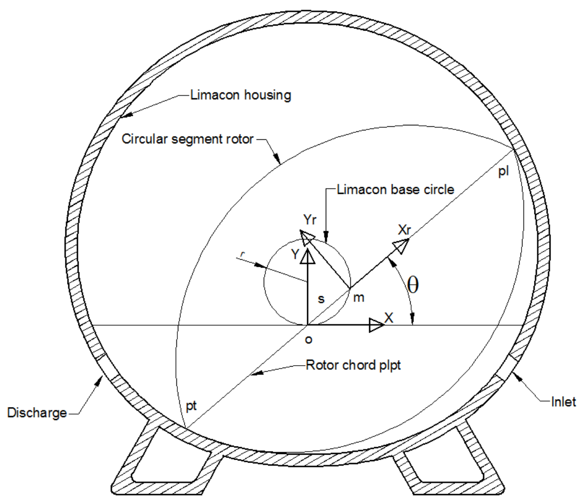

Figure 4: L2C expander [19]

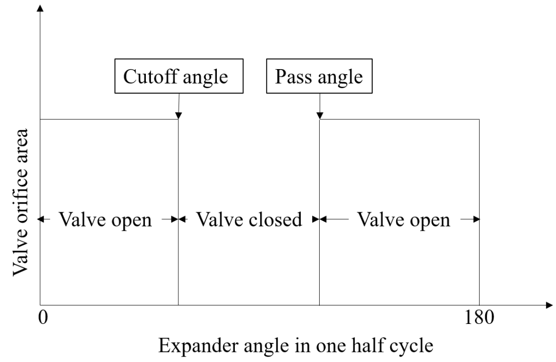

Figure 5: Ideal valve operation with reference to rotor angular position

from the measurement of speed of the rotor and fed to the motor controller. The controller will then be able to regulate the input phase voltages to the stepper motor according to the two objective angles as shown in Fig. 5 so that the rotary valve guided by the motor would be able to change its direction of rotation accordingly. Proper valve operation will ensure a controlled amount of compressed fluid is induced into the expander and in turn, increases system efficiency.

A. Dynamic response of DDRV

Equations (5), (6), (8) and (9) are solved iteratively with the parameters given in Table I using Matlab. The DDRV valve is actuated by applying a voltage input that produces currents in the windings as shown in Fig. 6a and 6b. The components of current in direct and quadrature (dq) axes is shown in Fig. 7. The q-axis component i_q contributes solely to the production of torque τ_e as seen in this figure. The resulting response curves of angular displacement, angular velocity, generated torque, valve opening and closing phases and flow rate through the valve port are calculated as shown in Fig. 8 to 12.

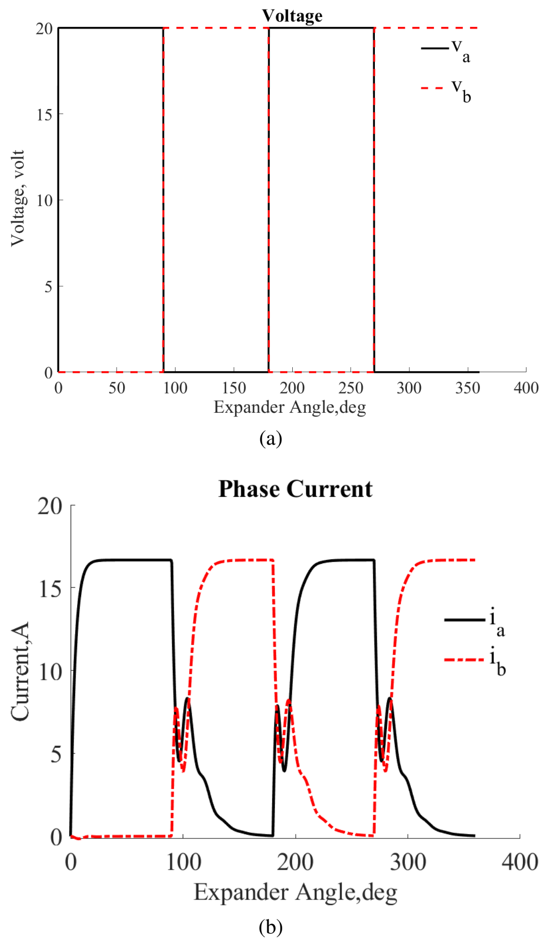

Figure 6: Input phase (a) voltage and (b) current

Table I: Data for the proposed valve

Number of phases	2
Phase voltages (V_a and V_b)	20 V
Step angle	10°
Winding self inductance (L_s)	1 mH
Winding resistance (R_s)	1.2 Ω
Maximum flux linkage (ψ_m)	0.04 V s
Viscous friction coefficient (B)	1×10^{-3} Nm s
Total moment of inertia (J)	5.47×10^{-6} kgm^2
Supply pressure (P_{in})	1000 kPa
Supply temperature (T_{in})	120 ° C
Valve ante-chamber pressure (P_a)	600 kPa
Expander speed	800 rpm
Diameter of orifice ($D_{orifice}$)	25 mm
Diameter of valve shaft (D_{valve})	15 mm
Discharge velocity coefficient (C_v)	0.98
Discharge coefficient (C_d)	0.65
Jet angle (α)	69°
Cutoff angle (θ_{cutoff})	90°
Pass angle (θ_{pass})	180°

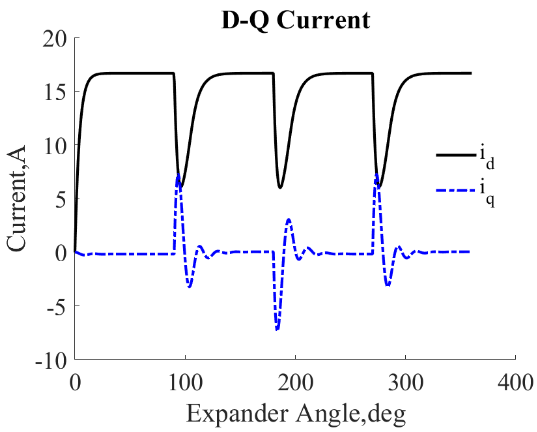

Figure 7: D-Q currents

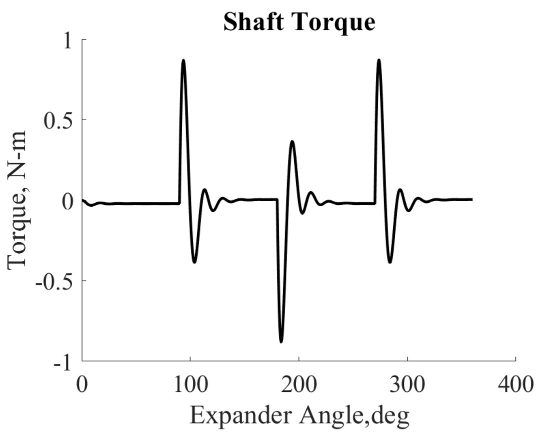

Figure 8: Torque produced by stepper motor

From Fig. 9a, it can be seen that a voltage input does not produce an instant response in the valve spool and lags the ideal response curve in the form of some delay. Fig. 9b shows a closing operation

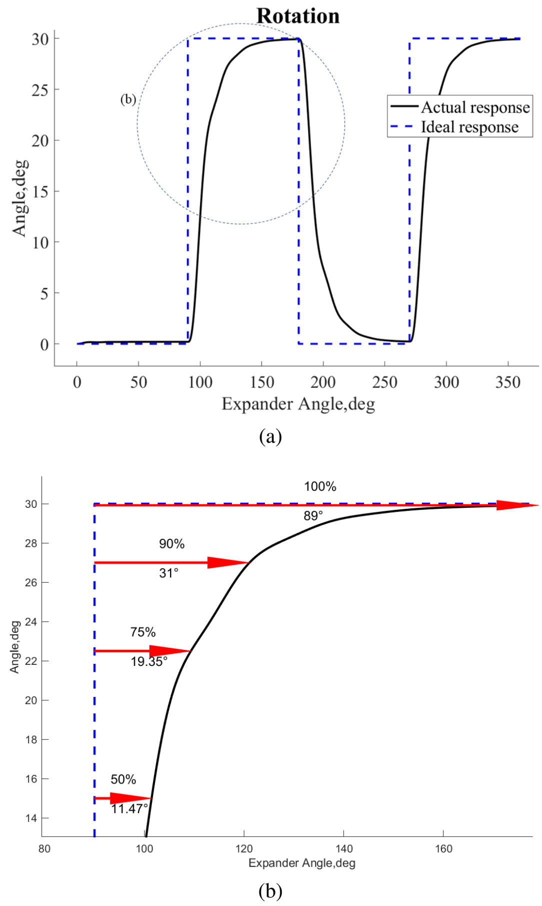

Figure 9: (a) Angular displacement of valve spool and (b) Delay in response

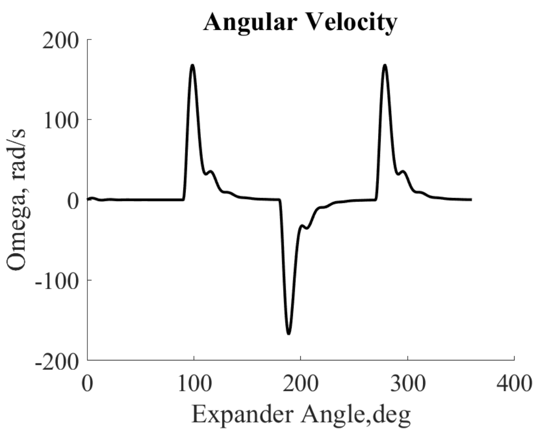

Figure 10: Angular velocity of valve spool

with delays in terms of expander angle. The valve spool keeps rotating for the total duration of the voltage input i.e., θ_{pass}. The valve response delay is relatively small at 11.47° for 50% closed position followed by a higher degree of delay as it gets closer to a fully closed position and roughly equals the closing duty cycle, $(\theta_{pass} - \theta_{cutoff})$. The delay can be adjusted by adjusting any or all of the parameters like the duty cycle, step angle and orifice diameter. The valve area and flow rate change in conformity to the angular displacement of the valve spool.

B. DDRV as an inlet control valve

The proposed DDRV is tested on an L2C expander as an inlet control valve. The mathematical model as proposed by Sultan [19] for the L2C expander is utilized for the purpose of this study. The expander is simulated for a full cycle of operation and the thermodynamic performance indicators such as energy, filling factor, isentropic efficiency, massflow and indicated power are calculated. Thermodynamic properties of the expander without any control

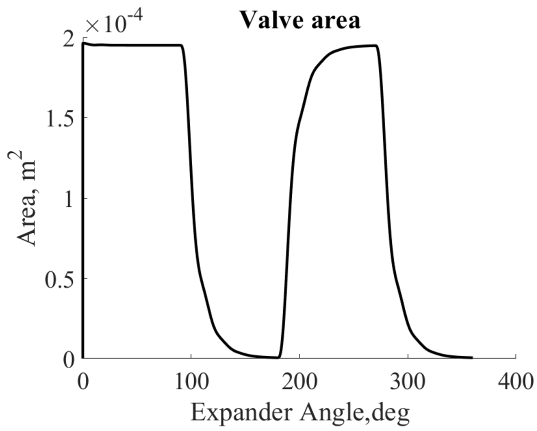

Figure 11: Valve area variation

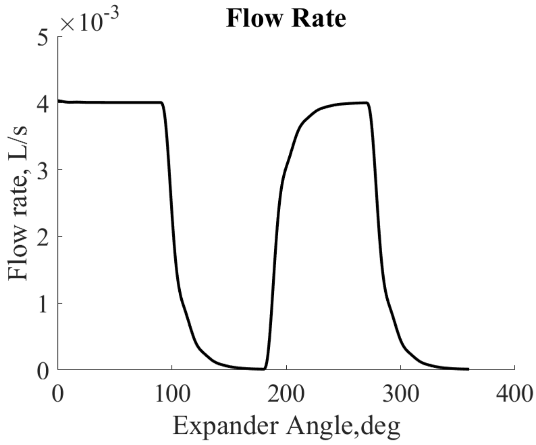

Figure 12: Flow rate

valve are also calculated and compared with the properties of the expander with the proposed valve in the inlet orifice. The pressure-volume (PV) diagram for the entire expansion cycle of the expander with and without an inlet valve is shown in Fig. 13. The gas is allowed to expand up to the chamber volume, $2.05 \times 10^{-4}\,\mathrm{m}^3$ as shown in Fig. 13. The thermodynamic performance of the expander with and without an inlet valve is shown in Fig. 14. The energy produced ($83.91\,\mathrm{Nm/rad}$) and indicated power ($1.12\,\mathrm{kW}$) output are higher without the valve compared to with a valve as the flow of compressed gas is not restricted. As such the massflow rate ($0.19\,\mathrm{kg/min}$) is higher in this case. This in turns accounts for low isentropic efficiency (54.97%) and higher filling factor(0.77). On the contrary, expander with the DDRV has better performance in terms of isentropic efficiency (63.14%) and filling factor (0.64). The slight reduction in energy production and power output, in this case, is compensated by the isentropic efficiency and filling factor improvement.

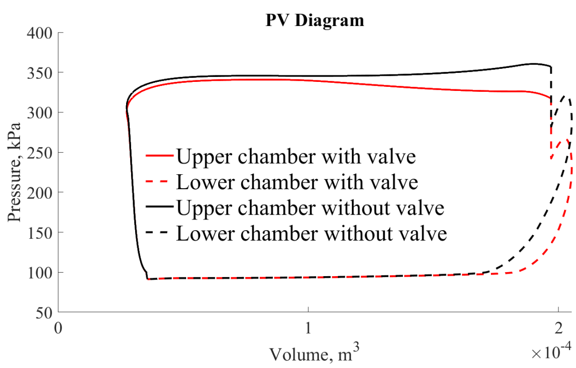

Figure 13: PV diagram

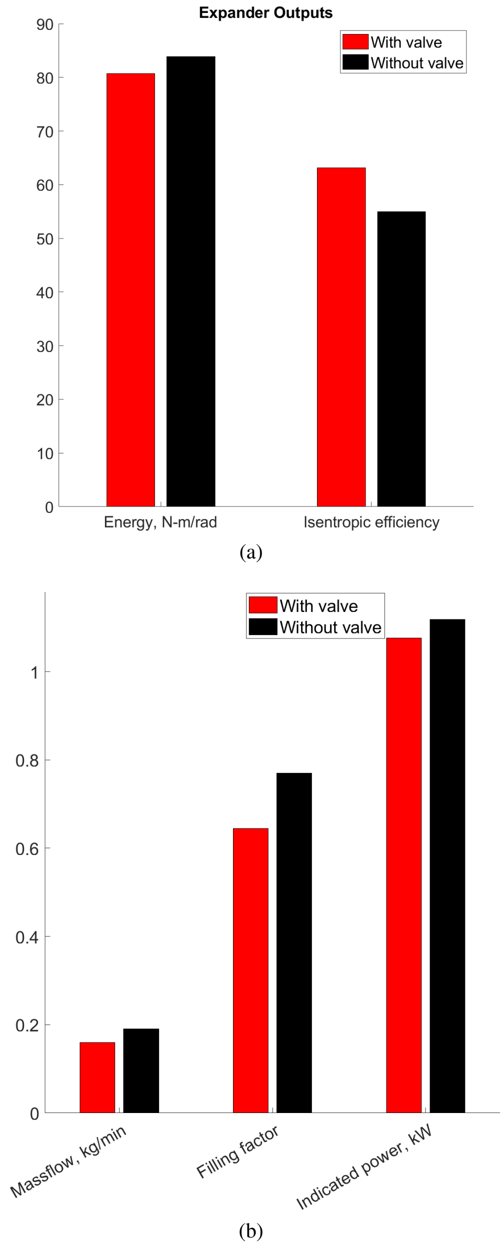

Figure 14: Expander outputs (a) energy and isentropic efficiency; (b) massflow, indicated power and filling factor

V. Results and Discussions

Simulation of DDRV as an inlet control valve of a gas expander provides key insights into the dynamic performance of the valve and ways to improve performance in control and operation. As seen in the previous section, the gas expander used in this study has a rotational speed of 800 rpm and the proposed valve should be able to open and close two times in each cycle of operation. This poses a tremendous challenge in satisfactory control and operation of DDRV. As seen from Fig. 6a, 6b and 9a, the valve is subjected to a delay between the instances input voltage is applied to the resulting buildup of current and mechanical displacement of motor rotor. This delay needs to be taken into account while designing a control system in future. Still, the proposed valve has a really high speed of response as seen in Fig. 10 and the torque produced as seen in Fig. 8 is also sufficient to actuate the valve against high pressure fluid flow. The proposed valve improves the overall performance of the L2C expander. An isentropic efficiency value of 63.14% is achieved which is an increase of 14.86% compared to an expander without a valve. Similarly, a filling factor value of just over 0.64 is achieved. Although, this has decreased about 16.88% compared to the ported operation of the expander, it is reasonable in terms of efficiency consideration. An indicated power of $1.07\,\mathrm{kW}$ and massflow rate of $0.16\,\mathrm{kg/min}$ is also achieved using DDRV. Optimisation of the proposed DDRV parameters along with expander characteristics can improve efficiency and filling factor further. This should yield better dynamic performance in future.

VI. Conclusion

Improving the efficiency of small-scale power-generating units such as the one discussed here can go a long way to mitigate the energy crisis and curve greenhouse gas emissions. The proposed valve has the potential to be a useful tool to improve the process efficiency of such systems. As shown above, just the introduction of the proposed DDRV can improve the isentropic efficiency of gas expansion process by at least 14.86% . This will subsequently improve the overall efficiency of such power generating units. Besides, the mathematical models and simulated responses provide necessary measures for future optimization and insights into the implementation of L2C expander based systems.

References

[1] G. Putrus and E. Bentley, "Integration of distributed renewable energy systems into the smart grid," in *Electric Renewable Energy Systems*, M. H. Rashid, Ed., Boston: Academic Press, 2016, pp. 487–518, ISBN: 978-0-12-804448-3. DOI: https://doi.org/10.1016/B978-0-12-804448-3.00020-7. [Online]. Available: https://www.sciencedirect.com/science/article/pii/B9780128044483000207.

[2] A. Auld, A. Berson, and S. Hogg, "Organic Rankine cycles in waste heat recovery: a comparative study," *International Journal of Low-Carbon Technologies*, vol. 8, no. $suppl_1$, pp. i9–i18, Jul. 2013, ISSN: 1748-1317. DOI: 10.1093/ijlct/ctt033. eprint: https://academic.oup.com/ijlct/article-pdf/8/suppl_1/i9/2316185/ctt033.pdf. [Online]. Available: https://doi.org/10.1093/ijlct/ctt033.

[3] G. Holdmann, "The Chena hot springs 400kW geothermal power plant: Experience gained during the first year of operation," *Transactions - Geothermal Resources Council*, vol. 31, Jan. 2008.

[4] A. Rentizelas, S. Karellas, E. Kakaras, and I. Tatsiopoulos, "Comparative techno-economic analysis of ORC and gasification for bioenergy applications," *Energy Conversion and Management*, vol. 50, no. 3, pp. 674–681, 2009, ISSN: 0196-8904. DOI: https://doi.org/10.1016/j.enconman.2008.10.008. [Online]. Available: https://www.sciencedirect.com/science/article/pii/S0196890408004160.

[5] S. Quoilin, M. S. Orosz, and V. Lemort, "Modeling and experimental investigation of an organic rankine cycle using scroll expander for small scale solar applications," *1st International Congress on Heating, Cooling, and Buildings*, 2008. [Online]. Available: https://orbi.uliege.be/bitstream/2268/1298/1/245.

[6] M. Kane, D. Larrain, D. Favrat, and Y. Allani, "Small hybrid solar power system," *Energy*, vol. 28, no. 14, pp. 1427–1443, 2003, ISSN: 0360-5442. DOI: https://doi.org/10.1016/S0360-5442(03)00127-0. [Online]. Available: https://www.sciencedirect.com/science/article/pii/S0360544203001270.

[7] X. Wang, L. Zhao, J. Wang, W. Zhang, X. Zhao, and W. Wu, "Performance evaluation of a low-temperature solar rankine cycle system utilizing R245fa," *Solar energy*, vol. 84, no. 3, pp. 353–364, 2010.

[8] E. B. L. Ksayer, "Design of an orc system operating with solar heat and producing sanitary hot water," *Energy Procedia*, vol. 6, pp. 389–395, 2011.

[9] A. Bademlioglu, A. Canbolat, N. Yamankaradeniz, and O. Kaynakli, "Investigation of parameters affecting organic rankine cycle efficiency by using Taguchi and ANOVA methods," *Applied Thermal Engineering*, vol. 145, pp. 221–228, 2018, ISSN: 1359-4311. DOI: https://doi.org/10.1016/j.applthermaleng.2018.09.032. [Online]. Available: https://www.sciencedirect.com/science/article/pii/S1359431118336834.

[10] I. A. Sultan, "Optimum design of limaçon gas expanders based on thermodynamic performance," *Applied Thermal Engineering*, vol. 39, pp. 188–197, 2012, ISSN: 1359-4311. DOI: https://doi.org/10.1016/j.applthermaleng.2012.01.039. [Online]. Available: https://www.sciencedirect.com/science/article/pii/S1359431112000580.

[11] I. A. Sultan, T. H. Phung, and A. Alhelal, "Improving process efficiency by waste heat recuperation : An application of the limaçon technology," *Sustainability in the Mineral and Energy Sectors*, pp. 475–498, Sep. 2016. DOI: 10.1201/9781315369853-25. [Online]. Available: https://www.taylorfrancis.com/chapters/edit/10.1201/9781315369853-25/improving-process-efficiency-waste-heat-recuperation-ibrahim-sultan-truong-phung-ali-alhelal.

[12] C.-K. Lai, B.-W. Lin, H.-Y. Lai, and G.-Y. Chen, "FPGA-based hybrid stepper motor drive system design by variable structure control," *Actuators*, vol. 10, no. 6, 2021, ISSN: 2076-0825. DOI: 10.3390/act10060113. [Online]. Available: https://www.mdpi.com/2076-0825/10/6/113.

[13] N. Matsui, M. Nakamura, and T. Kosaka, "Instantaneous torque analysis of hybrid stepping motor," *IEEE Transactions on Industry Applications*, vol. 32, no. 5, pp. 1176–1182, 1996. DOI: 10.1109/28.536880.

[14] N. A. Iqteit, K. Yahya, F. M. Makahleh, *et al.*, "Simple mathematical and simulink model of stepper motor," *Energies*, vol. 15, no. 17, 2022, ISSN: 1996-1073. DOI: 10.3390/en15176159. [Online]. Available: https://www.mdpi.com/1996-1073/15/17/6159.

[15] A. Fitzgerald, J. Charles Kingsley, and S. D. Umans, *Electric machinery*. McGraw-Hill, 2003.

[16] S.-M. Yang and E.-L. Kuo, "Damping a hybrid stepping motor with estimated position and velocity," *IEEE Transactions on Power Electronics*, vol. 18, no. 3, pp. 880–887, 2003. DOI: 10.1109/TPEL.2003.810836.

[17] I. Okhotnikov, S. Noroozi, P. Sewell, and P. Godfrey, "Evaluation of steady flow torques and pressure losses in a rotary flow control valve by means of computational fluid dynamics," *International Journal of Heat and Fluid Flow*, vol. 64, pp. 89–102, 2017, ISSN: 0142-727X. DOI: https://doi.org/10.1016/j.ijheatfluidflow.2017.02.005. [Online]. Available: https://www.sciencedirect.com/science/article/pii/S0142727X16303459.

[18] J. Watton, "Fundamentals of fluid power control," 2009. DOI: 10.1017/CBO9781139175241.

[19] I. Sultan, "A geometric design model for the circolimaçon positive displacement machine," *Journal of Mechanical Design*, vol. 130, Jun. 2008. DOI: 10.1115/1.2901143.